

Role of p38MAPK and oxidative stress in copper-induced senescence

Emmanuelle Boilan · Virginie Winant ·
Elise Dumortier · Jean-Pascal Piret ·
François Bonfitto · Heinz D. Osiewacz ·
Florence Debacq-Chainiaux · Olivier Toussaint

Received: 17 July 2012 / Accepted: 8 March 2013 / Published online: 12 April 2013
© American Aging Association 2013

Abstract In the present work, we indicate that copper is involved in the senescence of human diploid fibroblasts and we describe mechanisms to explain it. Using different techniques, we show for the first time an accumulation of copper in cells during replicative senescence. This accumulation seems to be co-localized with lipofuscin. Second, we observed that an incubation of cells with copper sulfate induced oxidative stress, antioxidant response and premature senescence. Antioxidant molecules reduced the appearance of premature senescence. Third, we found that Nrf2 transcription factor was activated and regulated the expression of genes involved in antioxidant response while p38^{MAPK} regulated the appearance of premature senescence.

Keywords Aging · Senescence · Copper · Metals · p38^{MAPK} · Oxidative stress · Human fibroblasts

Electronic supplementary material The online version of this article (doi:10.1007/s11357-013-9521-3) contains supplementary material, which is available to authorized users.

E. Boilan · V. Winant · E. Dumortier · J.-P. Piret ·
F. Bonfitto · F. Debacq-Chainiaux · O. Toussaint (✉)
NARILIS URBC, University of Namur (FUNDP),
61, rue de Bruxelles,
5000 Namur, Belgium
e-mail: olivier.toussaint@fundp.ac.be

H. D. Osiewacz
Institute of Molecular Biosciences,
Johann Wolfgang Goethe University,
Frankfurt am Main, Germany

Introduction

Hayflick showed that human diploid fibroblasts (HDFs) undergo a limited number of population doublings in culture before irreversible growth arrest and called it replicative senescence (RS) (Hayflick and Moorhead 1961). Cells in RS are characterized by an enlarged morphology, increased production of reactive oxygen species (ROS), accumulation of lipofuscin, mitochondrial alterations, lysosomal alterations like senescence associated β -galactosidase activity (SA- β gal) and a modified expression of several senescence associated genes (Campisi and d'Adda di Fagagna 2007). Acute and repeated exposure to oxidizing and/or DNA damaging agents at sublethal concentration may induce a senescent phenotype called stress-induced premature senescence (SIPS) with same markers appearing from 48 to 72 h after the last stress (Toussaint et al. 2000). p38 Mitogen-activated protein kinase (MAPK) is activated in RS and in premature senescence induced by oncogenic Ras, ultraviolet-B or H₂O₂ (Debacq-Chainiaux et al. 2010). Inhibition of p38^{MAPK} activity attenuates the increase in the proportion of SA- β gal positive cells and modifies the profiles of senescence-related gene expression in premature senescence induced by H₂O₂ (Zdanov et al. 2006).

Copper (Cu) is an essential micronutrient that plays a catalytic role in the activity of several enzymes through changes of its oxidation state (e.g. in cytochrome c oxidase) (Stern 2010). In addition, the redox chemistry of Cu also allows the generation of ROS

(Seth et al. 2004). Depending on their concentration and on the antioxidant capacities of the considered cell types, ROS participate in many physiological processes such as cellular signalling or generate oxidative stress that damages lipids, proteins or nucleic acids (Remacle et al. 1995). The antioxidant defences of aerobic organisms control uptake, distribution, detoxification or elimination of Cu, thus reducing the production of ROS catalyzed by Cu (Seth et al. 2004). Nuclear factor-erythroid 2-related factor 2 (Nrf2) is a major transcription factor involved in the expression of genes encoding for detoxifying enzymes such as NAD(P)H dehydrogenase quinone 1 (NQO1) or heme-oxygenase-1 (HO-1) (Kang et al. 2005). Cu and other heavy metals can activate Nrf2 responses (Simmons et al. 2011).

Recently, it became clear that Cu is implicated in age-associated disorders such as Alzheimer's disease and in the aging process (Brewer 2007). In the ascomycete *Podospora anserina*, a link between Cu and aging has been established (Borghouts et al. 2001). In old cultures of *P. anserina*, several changes occur which are referred to as the "senescence syndrome". This particularity makes this ascomycete a model organism to study mechanisms of aging. A decrease of Cu concentration in the culture medium of *P. anserina* results in lifespan extension. Also, an intracellular change in Cu distribution occurs and expression of some Cu-regulated genes increases during senescence of *P. anserina* (Osiewacz and Borghouts 2000). We showed that the mammalian homologues of these Cu-regulated genes are overexpressed in senescent WI-38 HDFs. Also, an increased Cu concentration in the culture medium of WI-38 HDFs seemed to lead to the appearance of some biomarkers of senescence (Scheckhuber et al. 2009). These preliminary studies were the first evidence that Cu could be implicated in senescence in human cells. Other authors confirmed the ability of Cu to induce premature senescence in HDFs (Matos et al. 2012).

In the present work, first we assayed cellular Cu levels during replicative senescence and after copper sulfate (CuSO_4) incubation in WI-38 HDFs with different techniques. Second, we tested whether CuSO_4 incubation induced the appearance of SIPS by an oxidative stress. We studied the implication of Nrf2 and p38^{MAPK} pathways in the Cu-induced oxidative stress and tested a possible role of p38^{MAPK} in the Cu-induced premature senescence.

Methods

Cell culture and exposure to CuSO_4

WI-38 fetal lung HDFs (American Type Culture Collection, #CCL-75, USA) were cultivated as described in Scheckhuber et al. (2009). Cells unable to complete a population doubling within 2 weeks were considered as replicatively senescent. Young and senescent WI-38 HDFs used for experiments were respectively at 60 % and 95 % of in vitro proliferative lifespan (27 or 43 population doublings).

Sub-confluent young WI-38 HDFs were subplated at 14,000 cells/cm² in Basal Medium Eagle (BME, Gibco Life Technologies, USA) + 10 % fetal bovine serum (FBS, Gibco Life Technologies, USA). At 24 h after seeding, the cells were incubated in culture medium with 500 μM of CuSO_4 ($\text{CuSO}_4 \cdot 5\text{H}_2\text{O}$, UCB, Belgium) for 16 h in cell incubator (HERAcell 240, Qlab, Belgium). Controls were incubated in BME + 10 % FBS. After treatment, the cells were washed once with phosphate buffer saline (10 mM phosphate, 155 mM NaCl, pH 7.4 (PBS), Lonza, Belgium) and incubated with BME + 10 % FBS.

Intracellular Cu assay

WI-38 HDFs were washed once with PBS, incubated with trypsin for 10 min, resuspended in PBS, counted with Neubauer chamber and centrifuged at 1,000 rpm for 5 min to collect cells. Cells were lysed with NaOH 0.5 N for 30 min with agitation on a shaking plate. The samples were boiled at 100 °C for 30 min before assaying intracellular Cu (QuantiChrom copper assay kit, BioAssay Systems, USA) following the instructions. The amount of proteins was assayed using the Pierce method (Sigma, USA). Triplicates were performed.

Intracellular Cu localization by fluorescent dye Coppersensor-1

The Coppersensor-1 (CS1) was developed and kindly provided by Christopher J Chang, Department of Chemistry, University of California at Berkeley. WI-38 HDFs seeded on glass cover slides were washed with PBS, incubated with CS1 at 10 μM in BME + 10 % FBS for 20 min, washed with PBS and fixed for 10 min with 4 % paraformaldehyde (Merck, Germany). After three

washings with freshly prepared PBS, glass cover slides were mounted in Mowiol (Molecular Probes, USA) and were incubated overnight at 4 °C. The cells were analyzed using a TCD confocal laser microscope (Leica, Germany) equipped with appropriate filters. Triplicates were performed.

Intracellular Cu localization by rubeanic acid method

For stock solution of rubeanic acid, we dissolved 50 mg of rubeanic acid in 50 mL of absolute ethanol. For working solution of rubeanic acid: 2.5 mL of stock solution in 50 mL of sodium acetate, 10 % aqueous. WI-38 HDFs were washed once by PBS, fixed for 10 min using 4 % paraformaldehyde (Merck, Germany), incubated with the working solution of rubeanic acid overnight at 37 °C, incubated with 70 % ethanol for 15 min and with absolute ethanol for 6 h, washed with tap water and observed under an optical microscope.

Transmission electron microscopy + energy dispersive X-ray spectroscopy

WI-38 HDFs were treated as described in (Scheckhuber et al. 2009) and samples were prepared for transmission electron microscopy (TEM) (JEOL 7500F, acceleration voltage of 15 kV). For intracellular Cu detection, the electron microscope, able to work in Z-contrast imaging analysis, was coupled to an energy dispersive X-ray spectroscopy (EDX) detector for the analysis of the qualitative and quantitative elementary composition.

Detection of lipofuscin by Ziehl–Neelsen modified method

Carbol fuchsin (1 g of basic fuchsin dissolved in 10 mL absolute ethanol and 100 mL of 5 % aqueous phenol) is mixed well for several hours and filtered before use. WI-38 HDFs were washed once with PBS, fixed for 10 min using 4 % paraformaldehyde (Merck, Germany), incubated with carbol fuchsin overnight at room temperature, washed once with tap water and incubated with acid alcohol (1 % HCl, 100 % alcohol) until excess background staining is removed. Cells were washed once with tap water, once with alcohol, once with tap water and observed under an optical microscope.

SA-βgal and [³H]-thymidine incorporation

Cells were seeded in 6-well culture plates at 20,000 cells/well at 24 h after the end of the CuSO₄ incubation. SA-βgal was determined 48 h later, as described in Scheckhuber et al. (2009). The population of SA-βgal positive cells was determined by counting 400 cells per well. The proportion of positive cells is given as the percentage of total number of cells counted in each well. Triplicates were performed.

Cells were seeded in 24-well plates at 10,000 cells/well at 24 h after the end of the CuSO₄ incubation. At 24 h after seeding, cells were grown in 1 mL of BME + 10 % FBS supplemented with 1 μL [³H]-thymidine (specific activity: 2 Ci/mmol, DuPont NEN, USA) during 24 h in 5 % CO₂. After incubation, the cells were treated as described in Scheckhuber et al. (2009). Data were normalized to the cellular protein content assayed by Pierce method assay. Triplicates were performed.

RT-PCR

At different times after the end of the incubation, total RNA was extracted using the “TRI Reagent Solution” method (AB AM9738, Ambion, USA). Total RNA (2 μg) was reverse transcribed using a First Strand cDNA synthesis kit for real-time polymerase chain reaction (RT-PCR) (Roche, Switzerland). The PCRs were performed on 96-well plates (MicroAmp Optical Reaction Plate, Applied Biosystems, USA). The PCR amplification primers (IDT, USA and Applied Biosystems, USA) used are listed in Table S1 in [supplementary material](#). PCR mixture contained SYBR Green PCR Master Mix (Applied Biosystem, USA) and primers at optimal concentrations. A hot start at 95 °C for 5 min was performed, then 40 cycles at 95 °C for 15 s and 65 °C for 1 min using the ABI PRISM 7000 SDS Thermal Cycler (Applied Biosystems, USA). Triplicates were performed. The gene encoding for ribosomal highly basic 23-kDa (23 kDa, rb 23-kDa, RPL13A) protein was used as a housekeeping gene for semi-quantification by RT-PCR with the classical “ΔΔCT method”.

Measurement of ROS production with DCF-DA dye

At different times after the end of the incubation with CuSO₄, WI-38 HDFs were washed with PBS

supplemented with 10 μM of 2',7'-dichlorofluorescein diacetate (DCF-DA) (Invitrogen, UK) for 30 min in a cell incubator. Cells were incubated with fresh BME + 10 % FBS and the measure of fluorescence was performed by fluoroskan (Fluoroskan ascent Thermo Electron Corporation, Thermo Scientific USA) at 485 nm for excitation wavelength and 520 nm for emission wavelength. Fluorescence data were normalized to the cellular protein content assayed by the Pierce method after NaOH lysis. Triplicates were performed.

Confocal microscopy

WI-38 HDFs were seeded at 20,000 cells/cm² in full BME on a glass cover slide. At 24 h, the cells were incubated with CuSO₄. After 16 h of incubation with CuSO₄, the cells were washed with ice-cold PBS and fixed for 10 min using 4 % paraformaldehyde (Merck, Germany). After three washings with freshly made PBS, cells were permeabilized with Triton X-100 1 % (Merck, Germany) + PBS for 5 min at room temperature. After three washings in PBS containing 2 % of Bovine Serum Albumin (BSA) (Sigma, USA), cells were incubated with the primary antibody in PBS–BSA 2 %. The antibodies used are listed in Table S2 in the [supplementary material](#). After incubation, the cells were washed three times with PBS–BSA 2 %. The binding of antibodies was visualized using secondary antibodies coupled with Alexa Fluorescent dye 488 nm (Molecular Probes, USA, listed in Table S2 in the [supplementary material](#)). After three washings with PBS–BSA 2 % and one with PBS, nuclei were marked with TO-PRO-3 (Molecular Probes, USA) and the cells were washed three times with PBS. Coverslips were mounted in Mowiol (Molecular Probes, USA) and were incubated overnight at 4 °C. The cells were analyzed using a TCD confocal laser microscope (Leica, Germany) equipped with appropriate filters. Triplicates were performed.

Extraction of proteins

Extraction of total proteins was performed at different times after the end of the incubation with CuSO₄. WI-38 HDFs were washed with ice-cold PBS and scrapped in ice-cold lysis buffer (40 mM Tris pH 7.5, 150 mM KCl, 1 mM EDTA, 1 % Triton X-100) containing a protease inhibitor cocktail (“Complete” from Roche, Switzerland; one tablet in

2 mL of H₂O, added at a 1:25 dilution) and phosphatase inhibitors (25 mM NaVO₃, 250 mM PNPP, 250 mM α -glycerophosphate and 125 mM NaF, at a 1:25 dilution). The lysates were sonicated for 5 min and centrifuged at 13,000 rpm for 5 min, the supernatants were collected and frozen at –80 °C.

Extraction and separation of nuclear and cytoplasmic proteins were performed just after the end of incubation with CuSO₄ in 75-cm² flasks. Cells were washed with PBS containing 1 mM Na₂MoO₄ and 5 mM NaF, incubated on ice for 8 min with 10 mL cold hypotonic buffer (HB, 20 mM HEPES, 5 mM NaF, 1 mM Na₂MoO₄, 0.1 mM EDTA) and scrapped in 100 μL of HB containing 0.2 % NP-40 (Sigma, USA), a protease inhibitor cocktail (1:25) and phosphatase inhibitors (1:25). Lysates were centrifuged 30 s at 13,000 rpm. Sedimented nuclei were resuspended in 15 μL HB containing 20 % glycerol and protease/phosphatase inhibitors. Extraction was performed for 30 min at 4 °C by the addition of 15 μL HB containing 20 % glycerol, 0.8 M NaCl and protease/phosphatase inhibitors.

Western blot analysis

Proteins were assessed (Pierce method, Sigma, USA) before electrophoresis. Ten microgrammes of proteins (whole cell homogenate, nuclear or cytoplasmic fractions) were separated on standard NuPAGE 4–12 % Bis–Tris (MES) gels and SeeBlue Plus2 Pre-Stained Standard (Invitrogen #LC5925, UK). After migration, proteins were transferred to pure nitrocellulose membranes (Bio-Rad, USA) for Licor revelation. After a 2-h blocking in PBS and Licor blocking buffer (v/v) (Odyssey Infrared Imaging System Licor Biosciences, The Netherlands), the membrane was incubated with the primary antibody for 2 h in Licor blocking buffer–Tween 0.1 %. The antibodies used are listed in Table S2 in the [supplementary material](#). α -Tubulin was used as loading control for total and cytoplasmic fractions. Lamin B was used as loading control for nuclear fractions. After incubation, the membranes were washed with PBS–Tween 0.1 % for 5 min, four times. The membrane was incubated with the secondary antibody for 1 h, in Licor blocking buffer–Tween 0.1 %. The binding of antibodies was visualized using fluorescent probe-coupled secondary antibodies (anti-mouse, anti-rabbit, anti-goat (Odyssey Infrared Imaging System Licor Biosciences)) (Table S2 in [Supplementary Material](#)). After

incubation, the membrane was washed with PBS–Tween 0.1 % for 5 min, four times and PBS alone for 5 min, twice. Revelation of dried membrane was performed by Odyssey Infrared Imaging System Licor Biosciences software. Triplicates were performed.

DNA binding assay of Nrf2

DNA-binding assay using TransAM ELISA kit (Active Motif, USA) for detecting transcription factor DNA binding activity was performed according to the manufacturer's recommendations. Briefly, 10 µg of nuclear proteins was incubated for 2 h in a 96-well plate coated with a double-stranded oligonucleotide containing the consensus sequence recognized by Nrf2. The transcription factor bound to DNA was detected using a specific primary antibody (rabbit anti-Nrf2 H-300 SC-13032, Santa Cruz, USA) followed by an HRP-conjugated anti-rabbit IgG antibody. Absorbance was measured at 450 nm (Bio-Rad xMark Microplate Spectrophotometer, Bio-Rad USA).

Incubation with antioxidants

Antioxidants were used at respective concentrations of 100 µM 6-hydroxy-2,5,7,8-tetramethylchroman-2-carboxylic acid (Trolox, Sigma-Aldrich, USA) or 50 mM D-mannitol (Merck, Germany). At 24 h after seeding, cells were incubated with 50 mM mannitol and 500 µM CuSO₄ for 16 h. Trolox was never added in presence of CuSO₄ and was added after the end of incubation with CuSO₄. For the analysis of biomarkers of senescence, WI-38 HDFs were washed once with PBS and incubated with fresh BME + 10 % FBS supplemented or not with 100 µM Trolox or 50 mM mannitol for 72 h after end of incubation with CuSO₄.

Inhibition of p38^{MAPK}

p38^{MAPK} was inhibited using a specific inhibitor, SB203580 (Merck, Germany). At 24 h after seeding, WI-38 HDFs were incubated or not with 20 µM of SB203580 in BME + 10 % FBS supplemented or not with 500 µM of CuSO₄ for 16 h. For the analysis of biomarkers of senescence, WI-38 HDFs were washed once with PBS and incubated with fresh BME + 10 % FBS supplemented with p38^{MAPK} inhibitor or not for 72 h after the end of the incubation with CuSO₄.

Nrf2 siRNA transfection

Cells were incubated with siRNA corresponding to the human Nrf2 (*NFE2L2*) gene (SMARTpool siRNA M-003755-02-0010), Dharmacon, UK) or siRNA negative control non-targeting smart pool for non-specific effects for 24 h (Dharmacon, cat. #D-001206-13-20, UK). Dharmafect was used as a transfection reagent, following the manufacturer's instructions. Cells were seeded at 12,000 cells/cm². siRNAs were mixed with Opti-MEM medium (Gibco, UK) and BME + 10 % FBS to obtain a final concentration of 20 nM. After 24 h of siRNA incubation at 37 °C and 5 % CO₂, the cells were washed with PBS and the medium was changed for BME + 10 % FBS.

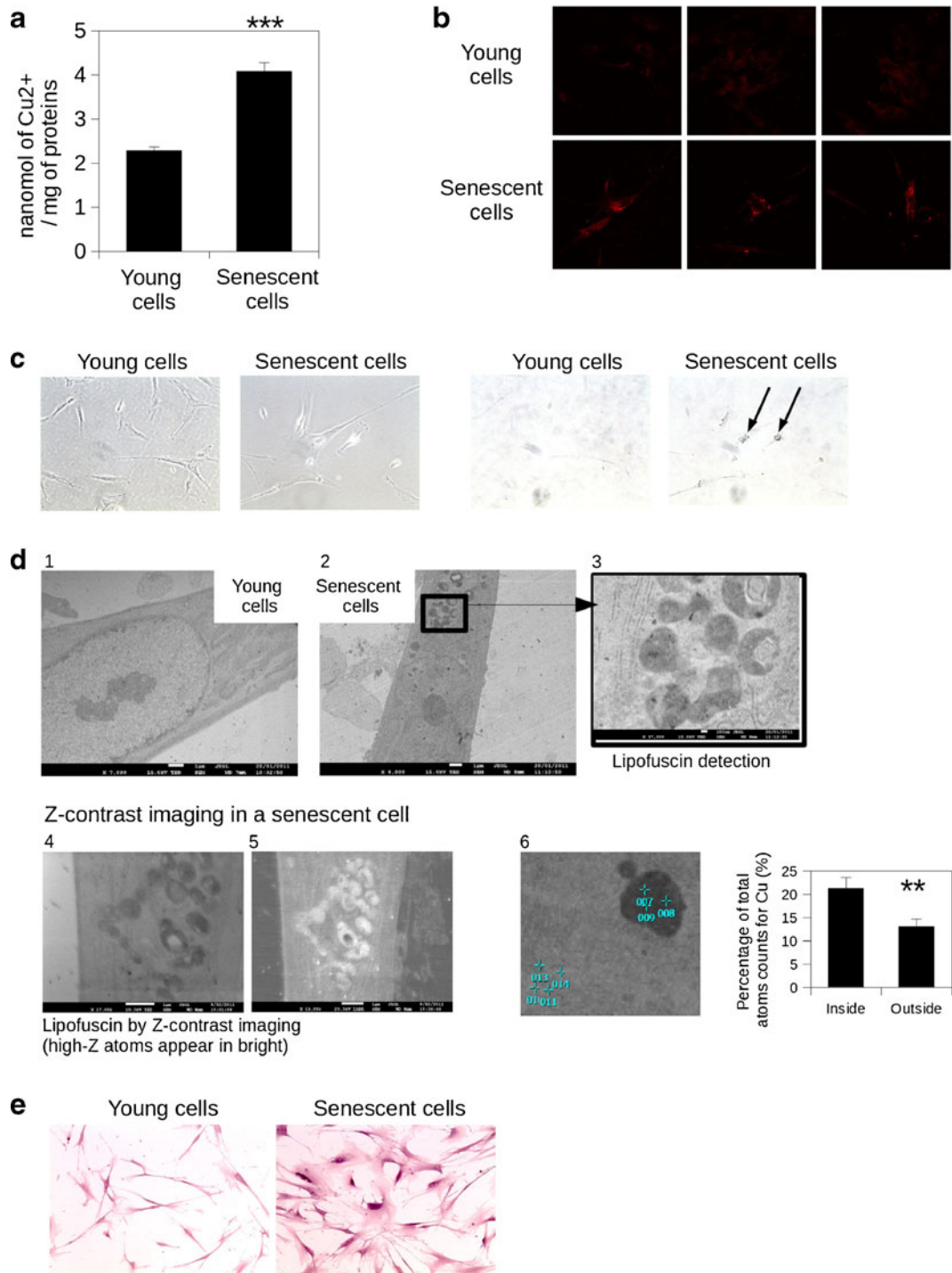
Statistical analysis

Statistical analysis was carried out with the Student's *t* test. Non-significant ($P > 0.05$); * $0.05 > P > 0.01$; ** $0.01 > P > 0.001$; *** $P < 0.001$.

Results

Accumulation of copper in RS of WI-38 HDFs

We used different methods to detect or assay intracellular Cu in WI-38 HDFs respectively at 60 % and 95 % of in vitro proliferative lifespan. First, we assayed intracellular Cu using the QuantiChrom copper assay utilizing a chromogen that forms a coloured complex specifically with copper ions. We found that Cu level was twofold higher in the senescent vs. young cells (Fig. 1a). Second, we detected intracellular Cu using a specific probe for Cu, Coppersensor-1 (CS1) (Zeng et al. 2006). CS1 is a membrane-permeable fluorescent dye for imaging labile Cu pools in cells and more particularly Cu⁺. The fluorescent signal corresponding to the intracellular Cu appeared higher in the senescent vs. young cells (Fig. 1b). Third, the rubanic acid method allowed detection of intracellular Cu deposits in young and senescent WI-38 HDFs. Black granules corresponding to Cu appeared only in senescent cells, and most of them were localized in the perinuclear zone (Fig. 1c) suggesting a potential co-localization of Cu and lipofuscin. Fourth, TEM allowed observation of multiple large granules in the senescent cells and not in the



young ones (Fig. 1d). These granules corresponded to lipofuscin granules as described in Jung et al. (2010). We used the Z-contrast imaging analysis to detect the high-Z atoms, represented in the majority by metal

atoms. We showed that lipofuscin granules appear in bright suggesting the presence of metals, which EDX identified as Cu. To do so, several areas inside a granule and several areas outside a granule were

Fig. 1 Accumulation of copper in RS of WI-38 HDFs. **a** Intracellular Cu assay in young and senescent WI-38 HDFs using a QuantiChrom Cu assay kit. The results expressed in nanomole of Cu^{2+} /milligramme of protein are given as mean \pm S.D. from three independent experiments. Statistical analysis: Student's *t* test. *** $P < 0.001$. **b** Intracellular Cu visualization in young and senescent WI-38 HDFs using Coppensor-1. The results are representative of three independent experiments. Magnification, $\times 100$. **c** Intracellular Cu detection in young and senescent WI-38 HDFs using Howell's rubeanic acid method. Magnification, $\times 100$. The results are representative of three independent experiments. **d** Intracellular Cu and lipofuscin detection in young and senescent WI-38 HDFs using TEM + EDX and Z-contrast imaging analysis. Magnification for image 1: $\times 7,000$; for image 2: $\times 6,000$; for image 3: $\times 37,000$; image 4: $\times 17,000$; image 5: $\times 13,000$ and image 6: $\times 40,000$. The graph represents the percentages of total Cu atoms counts inside and outside granules counted by EDX. Counts for carbon was used as atoms reference. **e** Lipofuscin detection in young and senescent WI-38 HDFs using the Ziehl–Neelsen modified method. Magnification, $\times 100$

selected in the cytoplasm of senescent cells. The EDX analysis showed a twofold increase of Cu levels inside vs. outside granules (Fig. 1d). In this study, the reference chemical element was carbon and was present in the same order in the two types of areas. Lastly, we used the Ziehl–Neelsen modified method to detect the lipofuscin in young and senescent WI-38 HDFs. Fuschia granules appeared only in senescent cells (Fig. 1e).

Treatment with sublethal concentration of CuSO_4 increases intracellular copper

We determined the sublethal concentration of CuSO_4 in WI-38 HDFs with an MTT assay (in [Supplementary Material](#)) and we observed that a lethal concentration of CuSO_4 induced death by apoptosis in WI-38 HDFs (in [Supplementary Material](#)). The experimental model of sublethal exposure to CuSO_4 is depicted in Fig. 2a. Using the QuantiChrom copper assay, we assayed intracellular Cu in WI-38 HDFs treated with CuSO_4 . Just at the end of the treatment with CuSO_4 , the intracellular concentration of Cu was increased eightfold in the CuSO_4 -treated cells vs. control cells. At 72 h after the end of the treatment with CuSO_4 , the intracellular concentration of Cu returned to the level of control cells. We observed a small increase in CuSO_4 -treated cells, but this difference was no longer statistically significant (Fig. 2b). We detected intracellular Cu using the CS1 probe and the fluorescent signal corresponding to the intracellular Cu, it

appeared higher in CuSO_4 -treated cells vs. control cells just at the end of the treatment with CuSO_4 . At 72 h after the end of the treatment with CuSO_4 , the intracellular concentration of Cu was similar at the fluorescent signal of control cells (Fig. 2c). Using the rubeanic acid method, we detected that black granules appeared in the CuSO_4 -treated cells just after treatment. These granules were still slightly visible at 72 h after the end of the treatment with CuSO_4 (Fig. 2d). In a preliminary study using TEM + EDX analysis, we had already detected Cu in CuSO_4 -treated cells and observed black granules only within CuSO_4 -treated cells (Scheckhuber et al. 2009). We used the Ziehl–Neelsen modified method to detect the lipofuscin in WI-38 HDFs treated with CuSO_4 or not, just after and 72 h after the end of the treatment with CuSO_4 . Fuschia granules appeared within CuSO_4 -treated cells both directly after CuSO_4 treatment and at 72 h after the end of the treatment (Fig. 2e).

Treatment with sublethal concentration of CuSO_4 induces premature senescence

A preliminary study showed an increase of the proportion of cells positive for SA- β gal and growth arrest at 72 h after the end of the treatment with 500 μM CuSO_4 for 16 h (Scheckhuber et al. 2009). In the present study, we confirmed these results and we analyzed other biomarkers of senescence such as the senescence associated morphological changes and expression of genes known to be overexpressed in senescent cells at 72 h after the end of the treatment with CuSO_4 (Fig. 3).

The genes encoding cyclin-dependent kinase inhibitor 1A (p21^{Waf1}), cyclin-dependent kinase inhibitor 2A (p16^{ink4a}), transforming growth factor- β 1 (TGF- β 1), connective tissue growth factor (CTGF), insulin growth factor binding protein 3 (IGFBP3), apolipoprotein J (ApoJ), fibronectin (Fibro) and osteonectin (Osteo) are known to be overexpressed in senescent cells (Pascal et al. 2005). Using RT-PCR, we showed that the abundance of the mRNA of p21^{Waf1}, p16^{ink4a}, TGF- β 1, ApoJ and Fibro was increased in CuSO_4 -treated cells vs. control cells at 72 h after the end of the treatment with CuSO_4 . The abundance of the mRNA of CTGF and IGFBP3 were also increased in CuSO_4 -treated cells vs. control cells, but these variations were not statistically significant. Unexpectedly, the abundance of the mRNA of Osteo was decreased in CuSO_4 -treated cells suggesting a negative impact of copper on Osteo expression.

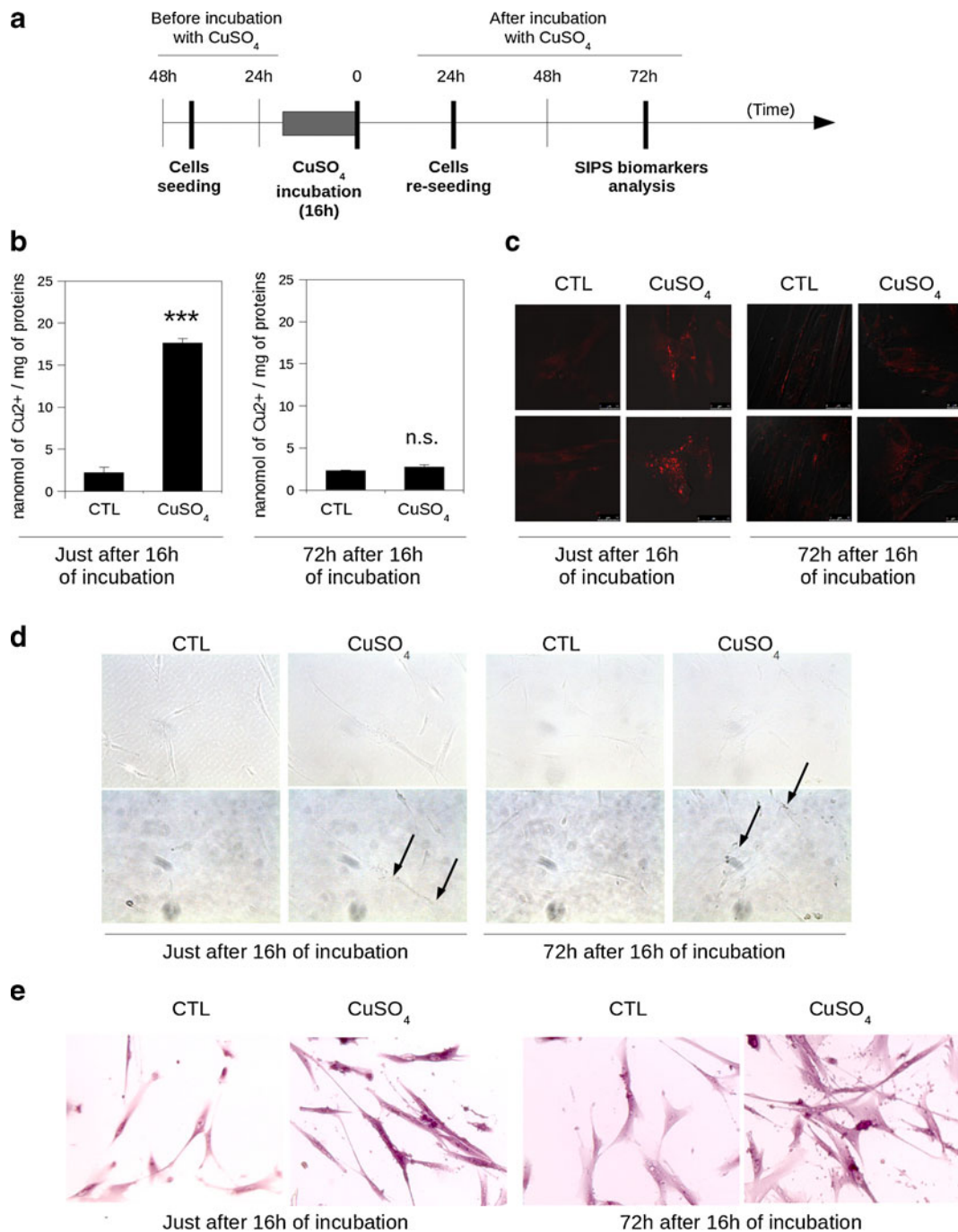


Fig. 2 Treatment with sublethal concentration of CuSO_4 increases intracellular copper. **a** Experimental design and time frame of CuSO_4 incubation. **b** Intracellular Cu assay in WI-38 HDFs just after the end and 72 h after the end of the treatment with 0 (CTL) or 500 μM CuSO_4 for 16 h using a QuantiChrom copper assay kit. The results expressed in nanomole of Cu^{2+} /milligramme of protein are given as mean \pm S.D. from three independent experiments. Statistical analysis: Student's *t* test. *ns* non-significant ($P>0.05$); *** $P<0.001$. **c** Intracellular Cu visualization WI-38 HDFs just after the end and 72 h after

the end of the treatment with 0 (CTL) or 500 μM CuSO_4 for 16 h using Coppensor-1. The results are representative of three independent experiments. **d** Intracellular Cu detection in WI-38 HDFs just after the end and 72 h after the end of the treatment with 0 (CTL) or 500 μM CuSO_4 for 16 h using the rubanic acid method. The results are representative of three independent experiments. Magnification, $\times 100$. **e** Lipofuscin detection in WI-38 HDFs just after the end and 72 h after the end of treatment with 0 (CTL) or 500 μM CuSO_4 for 16 h using the Ziehl–Neelsen modified method. Magnification, $\times 100$

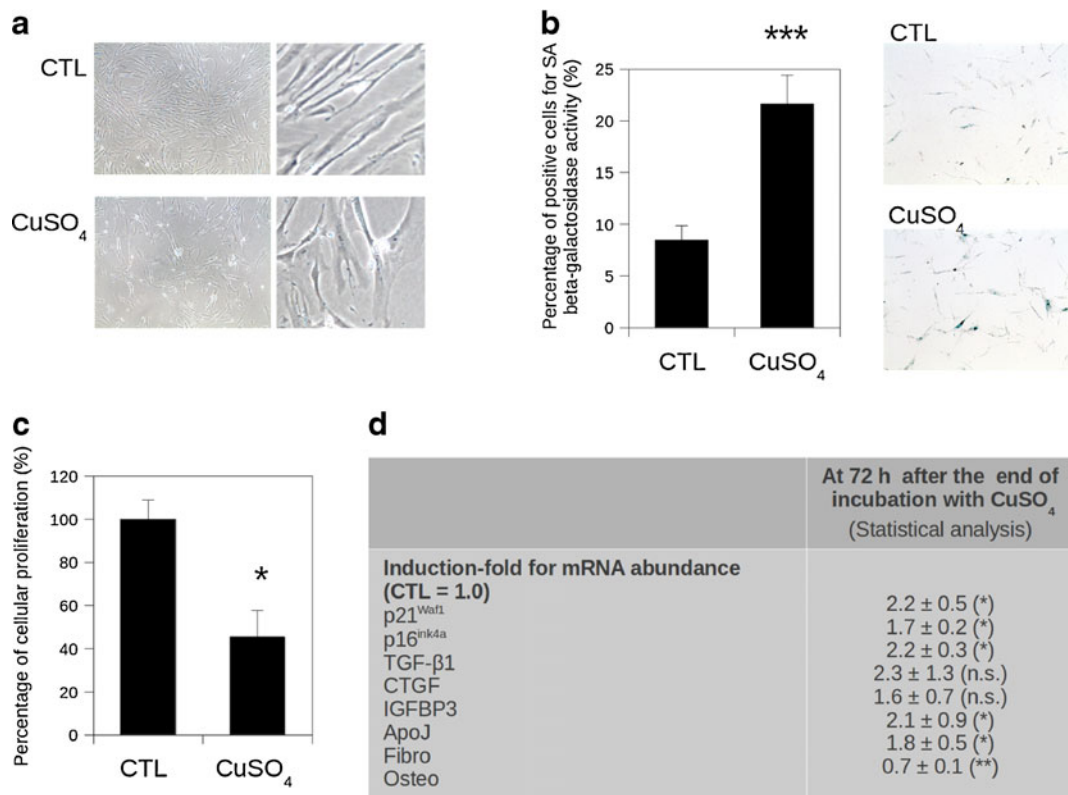


Fig. 3 Treatment with sublethal concentration of CuSO₄ induces premature senescence. The markers of senescence in WI-38 HDFs at 72 h after the end of the treatment with 0 (CTL) or 500 μM CuSO₄ for 16 h are presented. **a** Morphology of WI-38 HDFs at 72 h after the end of the treatment with 0 (CTL) or 500 μM of CuSO₄ for 16 h using optical microscope with phase contrast. Magnification, ×63. **b** Percentage of cells positive for SA-βgal at 72 h after the end of the treatment with 0 (CTL) or 500 μM of CuSO₄ for 16 h. The results are expressed in percentage of blue cells and are given as mean ± S.D. from three independent experiments. **c** Percentage of cellular proliferative potential corresponding to incorporation of

[³H]-thymidine in cells at 72 h after the end of the treatment with 0 (CTL) or 500 μM CuSO₄ for 16 h. The results are expressed in percentage compared to values for control cells (100 %) and are given as mean ± S.D. from three independent experiments. **d** mRNA abundance of senescence-associated genes using RT-PCR in cells at 72 h after the end of the treatment with 0 (CTL) or 500 μM CuSO₄ for 16 h. The results are expressed in fold induction of values for control cells (1.0) and are given as mean ± S.D. from three independent experiments. Statistical analysis: Student's *t* test. *ns* nonsignificant ($P > 0.05$); * $0.05 > P > 0.01$; ** $0.01 > P > 0.001$ and *** $P < 0.001$

Treatment with sublethal concentrations of CuSO₄ induces oxidative stress

We hypothesized that CuSO₄ can induce oxidative stress in WI-38 HDFs. First, we measured the production of ROS using 2',7'-dichlorofluorescein-diacetate (DCF-DA) dye in WI-38 HDFs treated or not with 500 μM CuSO₄ for 16 h. We demonstrated that CuSO₄ induced an increase of ROS production (Fig. 4a). WI-38 HDFs treated with 500 μM H₂O₂ for 2 h were used as positive control.

In nuclear and mitochondrial DNA, 8-oxo-7,8-dihydro-2'-deoxyguanosine (8-oxodG) is the most

frequent form of ROS-induced oxidative lesions and is widely used as a biomarker for oxidative stress. We detected 8-oxodG by immunofluorescence in WI-38 HDFs treated or not with 500 μM CuSO₄ for 16 h. We demonstrated that CuSO₄ induced an increase of the fluorescent signal corresponding at 8-oxodG (Fig. 4b).

Second, we studied the antioxidant response of Nrf2 and the detoxifying enzymes against oxidative stress such as HO-1 or NQO1. Using immunofluorescence, we showed that Nrf2 is translocated in the nucleus of WI-38 HDFs treated for 16 h with 500 μM CuSO₄ (Fig. 4c). We studied the potential DNA binding of Nrf2 using DNA-binding assays in

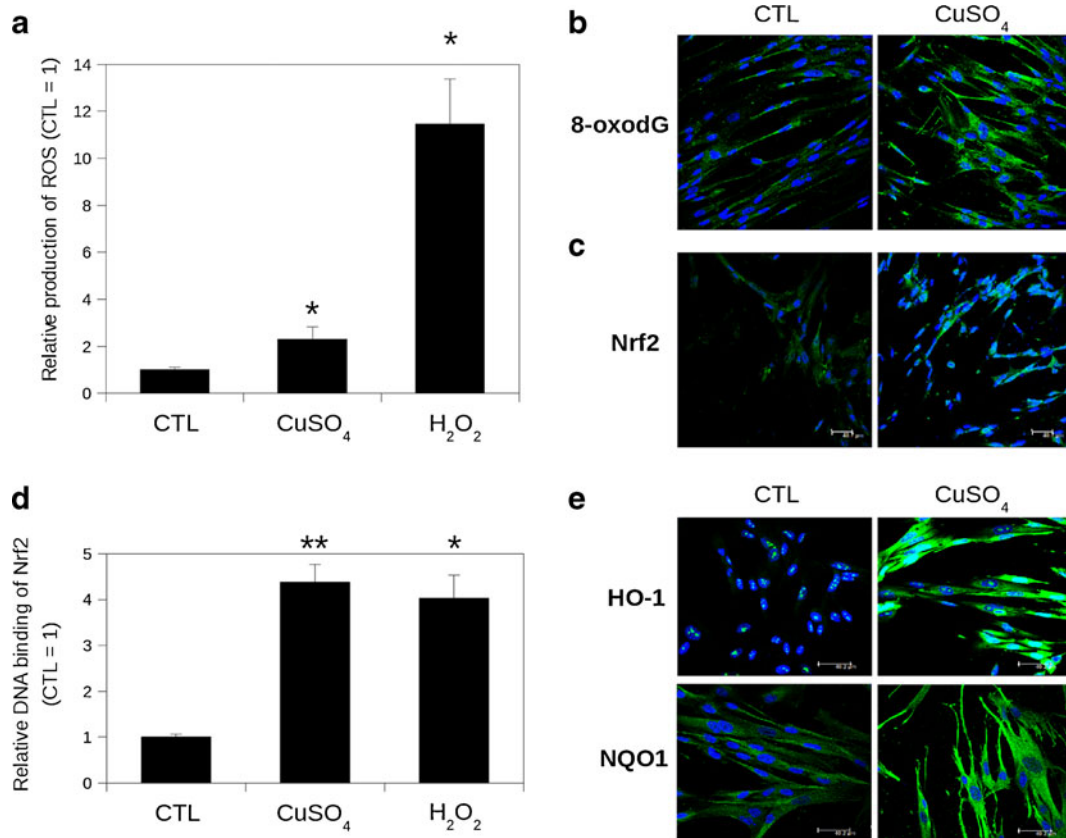


Fig. 4 Treatment with sublethal concentration of CuSO₄ induces oxidative stress. **a** Production of ROS in WI-38 HDFs at just after the end of the treatment with 0 (CTL) or 500 μM CuSO₄ for 16 h using DCF-DA dye. The results are expressed in induction fold of values for control cells and are given as mean ± S.D. from three independent experiments. Statistical analysis: Student's *t* test, *0.05 > *P* > 0.01. WI-38 HDFs treated with 500 μM of H₂O₂ for 2 h were used as positive control. **b** Immunofluorescence detection of 8-oxodG just after the end of the treatment with 0 (CTL) or 500 μM CuSO₄ for 16 h. TO-PRO-3 dye was used to detect nuclei. **c** Immunofluorescence detection of Nrf2 just after the end of the treatment with 0 (CTL) or 500 μM CuSO₄ for 16 h. TO-PRO-3

dye was used to detect nuclei. **d** DNA binding of Nrf2 in WI-38 HDFs just after the end of the treatment with 0 (CTL) or 500 μM CuSO₄ for 16 h using TransAM ELISA kit (Active Motif). The results are expressed as relative DNA binding activity of Nrf2 in comparison with control cells and are given as mean ± S.D. from three independent experiments. Statistical analysis: Student's *t* test, *ns* nonsignificant (*P* > 0.05); *0.05 > *P* > 0.01; **0.01 > *P* > 0.001. WI-38 HDFs treated with 500 μM H₂O₂ for 2 h were used as positive control. **e** Immunofluorescence detection of HO-1 and NQO1 just after the end of the treatment with 0 (CTL) or 500 μM CuSO₄ for 16 h. TO-PRO-3 dye was used to detect nuclei

these conditions. CuSO₄ induced a statistically significant increase in DNA-binding of Nrf2 (4.4-fold increase vs. control cells) (Fig. 4d).

We studied the abundance of the mRNA of HO-1, NQO1 and Nrf2 using RT-PCR. CuSO₄ induced a statistically significant increase of the abundance of the mRNA of HO-1, NQO1 and Nrf2: respectively 132.8 ± 54.8, 1.9 ± 0.3, 2.0 ± 0.4-fold vs. control cells.

At the protein abundance level, using immunofluorescence, we showed that CuSO₄ induced an increase

of fluorescent signal corresponding at HO-1, NQO1 (Fig. 4e) vs. control cells.

CuSO₄ induces premature senescence partially through oxidative stress

We hypothesized that CuSO₄ induces premature senescence through oxidative stress. WI-38 HDFs were incubated for 16 h with both 500 μM CuSO₄ and 50 mM mannitol, a radical scavenger (Desesso et al. 1994). Mannitol was also present in the culture

medium for 72 h after the end of the treatment with CuSO_4 . We measured the production of ROS using DCF-DA dye and subsequently we showed that the increase of ROS production by CuSO_4 was abolished by mannitol (Fig. 5a).

We analyzed the protein abundance of heat shock protein 70 or Hsp70 (a stress-induced protein), HO-1, NQO1 and Nrf2 by Western blot analysis. While CuSO_4 induced an increase of abundance of these proteins and increased the abundance of Nrf2 in the nucleus vs. control cells, there was a decreased abundance of Hsp70, HO-1, NQO1 in the total extract when cells were treated with CuSO_4 and mannitol (Fig. 5b). There is no significant variation for Nrf2 in the nucleus extracts for the same conditions. Quantification of bands from Western blot analysis is presented in [supplementary material](#).

The increase of the proportion of SA- β gal positive cells (Fig. 5c), and the decrease of proliferative potential (Fig. 5d) in WI-38 HDFs treated with CuSO_4 was confirmed. These modifications were less important in the presence of mannitol, but mannitol increased the proliferation of the control cells too.

Next, we confirmed these results using another antioxidant, 6-hydroxy-2,5,7,8-tetramethylchroman-2-carboxylic acid (trolox), a water-soluble derivative of vitamin E. Since the combination of trolox and CuSO_4 was cytotoxic (data not shown), trolox was added only after the end of the treatment with CuSO_4 for 72 h. The increase of the proportion of SA- β gal-positive cells (Fig. 5c) and the decrease of proliferative potential (Fig. 5d) were confirmed in WI-38 HDFs treated with CuSO_4 , and these variations were less important in the presence of trolox.

Phosphorylation of p38^{MAPK} is implicated in CuSO_4 -induced premature senescence

We hypothesized that p38^{MAPK} plays a role in premature senescence induced by CuSO_4 . We analyzed the abundance of phosphorylated p38^{MAPK} by Western blotting. Treatment of 16 h with 500 μM CuSO_4 induced an increase of abundance of phosphorylated p38^{MAPK} (Fig. 6a) vs. control cells. This increase was less important in the presence of 50 mM mannitol. Quantification of bands from Western blot analysis is presented in the [supplementary material](#).

We tested whether p38^{MAPK} plays a role in CuSO_4 -induced oxidative stress response using a selective

inhibitor of p38^{MAPK} activity SB203580. WI-38 HDFs were treated for 16 h with 500 μM CuSO_4 and 20 μM SB203580 or not. While CuSO_4 induced an increase of protein abundance for Hsp70, HO-1, NQO1 or Nrf2 (Fig. 6b) vs. control cells, these variations decreased for Hsp70 and HO-1 but not for NQO1 when cells were treated with both CuSO_4 and SB203580. The abundance of Nrf2 in the nucleus seemed similar in presence or not of p38^{MAPK} inhibitor. Quantification of bands from western-blot analysis is presented in [supplementary material](#).

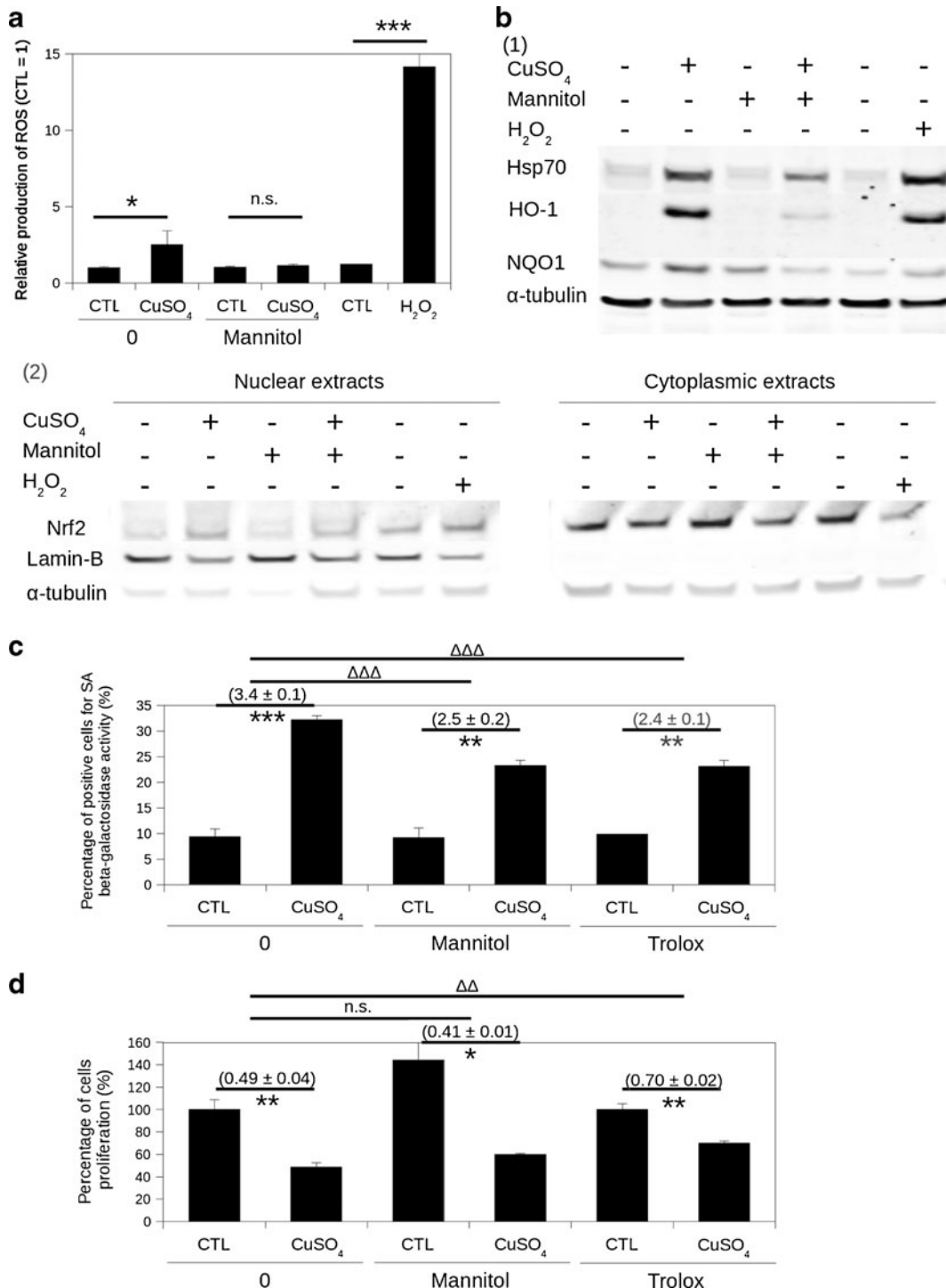
We studied the potential DNA binding of Nrf2 using DNA-binding assays in these conditions. CuSO_4 induced a statistically significant increase in DNA-binding of Nrf2 (2.1-fold increase vs. control cells) (Fig. 6c) and this seemed similar in the presence or absence of p38^{MAPK} inhibitor.

Of note, we checked whether Nrf2 regulates the abundance of HO-1, NQO1 and Hsp70 at mRNA in our model using Nrf2 targeting siRNA. While Nrf2 mRNA had virtually disappeared after transfection of the WI-38 HDFs with Nrf2 targeting siRNA, only a partial decrease was recorded for HO-1 (decrease from 270.5- to 88.9-fold of induction) and Hsp70 (from 201.4 to 93.3), which called for the intervention of another pathway, similar at least to p38^{MAPK} . For NQO1, the effect was nearly total (from 1.7- to 0.1-fold of induction). No effect was observed on senescence biomarkers (data not shown).

We also studied the implication of phosphorylated p38^{MAPK} in the appearance of biomarkers of senescence induced by CuSO_4 . WI-38 HDFs were treated for 16 h with 500 μM CuSO_4 and 20 μM SB203580 or not. SB203580 was also present in normal medium for 72 h after the end of the treatment with CuSO_4 . We confirmed that CuSO_4 induced an increase of the proportion of SA- β gal-positive cells and a decrease of proliferative potential in WI-38 HDFs treated with CuSO_4 . These CuSO_4 -induced variations were less important when SB203580 was present (Fig. 6d).

Discussion

An impact of copper on lifespan was earlier reported in the fungal aging model *P. anserina*. First, data came from the characterization of a long-lived mutant in which Cu-uptake is affected due to the loss of function mutation in a gene coding for the Cu dependent



transcription factor GRISA (Borghouts and Osiewacz 1998). In this mutant Cu uptake is defective due to impairments in the expression of a target gene of GRISA, *PaCtr3* encoding the Cu-transporter

PaCTR3. As a result, this mutant is depleted in cellular Cu and switches from a Cu-dependent cytochrome oxidase respiration to an iron-dependent alternative respiration (Osiewacz and Borghouts 2000). This type

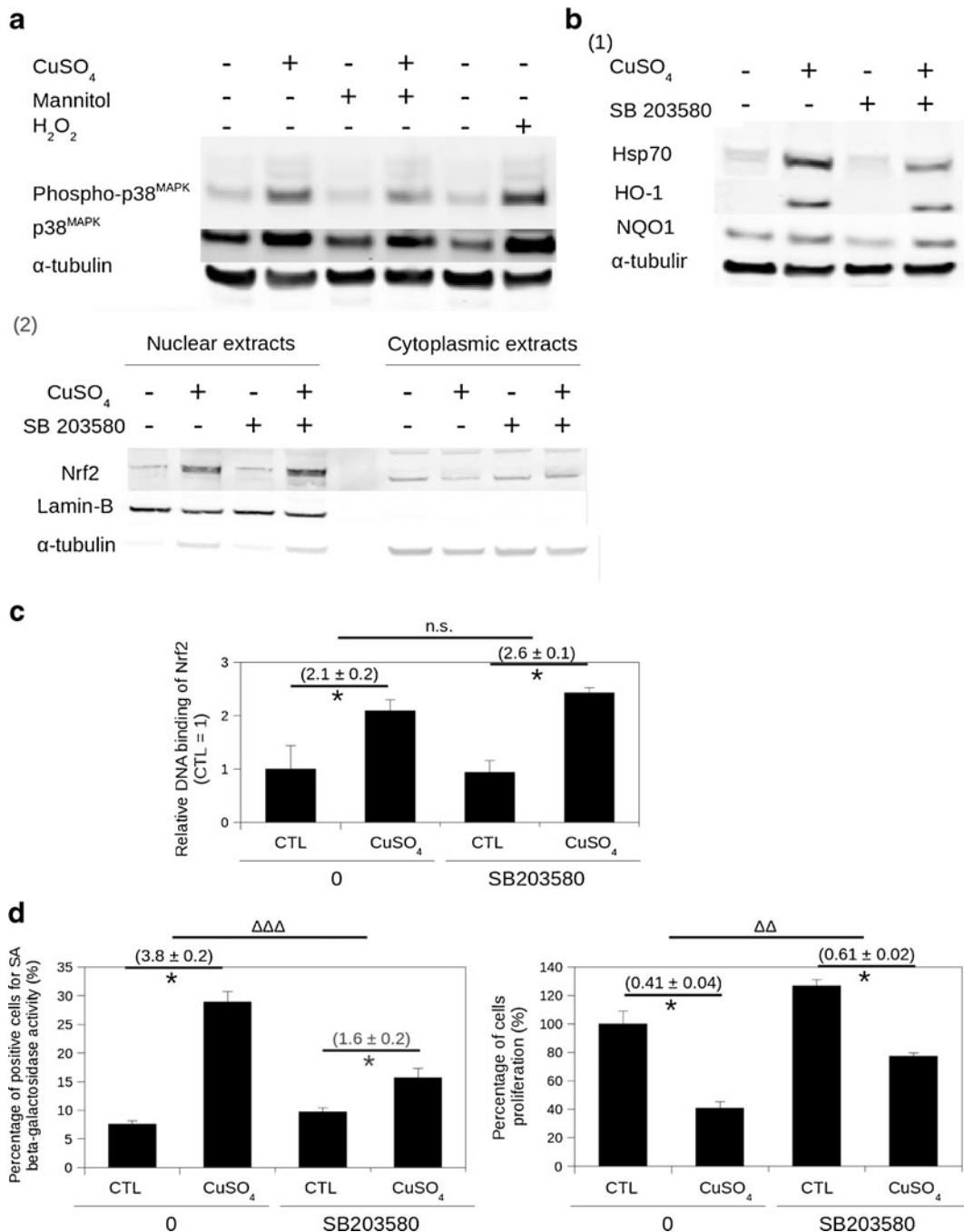
Fig. 5 CuSO₄ induces premature senescence through oxidative stress. **a** Production of ROS in WI-38 HDFs just after the end of the treatment with 0 (CTL) or 500 μM CuSO₄ and with 50 mM mannitol or not for 16 h using DCF-DA dye. The results are expressed in fold of values for control cells and are given as mean ± S.D. from three independent experiments. Statistical analysis: Student's *t* test, *n.s.* nonsignificant ($P>0.05$); $*0.05>P>0.01$; $***P<0.001$. WI-38 HDFs treated with 500 μM of H₂O₂ for 2 h were used as positive control. **b** Western blot analysis of Hsp70, HO-1, NQO1 (1) and Nrf2 (2) just after the end of the treatment with 0 (CTL) or 500 μM CuSO₄ and with 50 mM mannitol or not for 16 h. Ten microgrammes of protein from whole cell homogenate (1) or from the nuclear or cytoplasmic fractions (2) are used for the analysis. α-Tubulin and lamin-B were used as control loading. WI-38 HDFs treated with 500 μM of H₂O₂ for 2 h were used as positive control. **c** Percentage of SA-βgal positive in WI-38 HDFs at 72 h after the end of the treatment with 0 (CTL) or 500 μM CuSO₄ for 16 h and with antioxidant (50 mM mannitol or 100 μM trolox) or not. The results are expressed in percentage and are given as mean ± S.D. from three independent experiments. The numbers in the chart represent ratios between CTL and CuSO₄-treated cells and are given as mean ± S.D. from three independent experiments. Statistical analysis: Student's *t* test. $**0.01>P>0.001$; $***P<0.001$. The symbol Δ represents a statistical analysis between ratios. **d** Percentage of cellular proliferative potential (incorporation of [³H]-thymidine) in WI-38 HDFs at 72 h after the end of the treatment with 0 (CTL) or 500 μM CuSO₄ for 16 h with antioxidant (50 mM mannitol or 100 μM trolox) or not. The results are expressed in percentage (CTL = 100 %) and are given as mean ± S.D. from three independent experiments. The numbers in the chart represent ratios between CTL and CuSO₄-treated cells and are given as mean ± S.D. from three independent experiments. Statistical analysis: Student's *t* test. $*0.05>P>0.01$; $**0.01>P>0.001$. The symbol Δ represents a statistical analysis between ratios

of respiration leads to a lowered generation of ROS by the mitochondrial respiratory chain (Gredilla et al. 2006). Moreover, in wild-type strains of *P. anserina*, Cu was found to increase in the cytoplasm during aging leading to the activation of the Cu-related proteins (Scheckhuber et al. 2009).

In mammals, Cu accumulation was found to occur in bovine (Zatta et al. 2008) and human brain (Vasudevaraju et al. 2010) with age. Moreover, intracellular accumulation of Cu in Wilson's disease is due to inherited mutations of a nuclear gene encoding a Cu transporter, causing accumulation of Cu in the liver, particularly within the mitochondria. This accumulation of Cu within the hepatic mitochondria may cause premature oxidative aging molecular damage (e.g. of mitochondrial DNA) (Mansouri et al. 1997). Many investigations of brain and neuronal cells implicated Fe and Cu in the development of age-related diseases and in particular age-related neurodegenerative

diseases, via the capacities of these metals to generate ROS through the Fenton and Haber–Weiss reactions (Brewer 2007). Very few studies addressed the accumulation of these metals in senescent cells of peripheral tissues and the implication of these metals in the mechanisms of senescence of human cells. HDFs are an example of cells originating from peripheral tissues. Killilea et al. showed that total Fe content increases exponentially during cellular RS of IMR-90 HDFs. The total Fe content becomes tenfold higher vs. young cells (Killilea et al. 2004).

In this study, we showed with fluorescence-based (CS1) or cytochemistry-based (rubeanic acid) detection methods and with assays that intracellular Cu accumulates during RS of WI-38 HDFs, through unknown mechanisms and kinetics. We demonstrated that intracellular Cu was concentrated as granules in senescent cells, suggesting that intracellular Cu was associated with lipofuscin. We confirmed the accumulation of lipofuscin granules in cells during RS using TEM and a cytochemical method (basic fuchsin). Cu and lipofuscin seemed to co-localize within cells. The age-related intracellular accumulation of lipofuscin, especially in the lysosomal compartment, corresponds to protein material that accumulates during the aging process. In 2010, Höhn et al. demonstrated that cytotoxicity of lipofuscin is proportional with its ability to incorporate transition metals such as Cu and Fe (Höhn et al. 2010). These transition metals catalyzed the Fenton reaction and generated oxidative stress in cells, probably inducing a form of SIPS. Lipofuscin forms have been observed in Cu-charged hepatocytes of Wilson's disease patient, and Cu grains were observed in these cells (Motonishi et al. 2006). Terman et al. proposed that in senescent cells, the inability of autophagy and other cellular degradation mechanisms to eliminate damaged structures, generates a progressive accumulation of 'garbage', including cytosolic protein aggregates, defective mitochondria and lipofuscin (Terman et al. 2010). The slow accumulation of lipofuscin seems to adversely affect autophagy, resulting in a decreased turnover of effective mitochondria. The defective and enlarged mitochondria producing a greater amount of ROS are not eliminated. They constitute a growing population of badly functioning organelles, favouring lipofuscin accumulation. Vasudevaraju et al. demonstrated a clear correlation between Cu and Fe levels vs. strand breaks in aging brain regions (Vasudevaraju et al. 2010). In our model,



one can speculate that as Cu gradually accumulates in cells, DNA damage accumulates too, diminishing the proliferative potential of the HDFs and may participate in cellular senescence.

Prior to the study of senescence, we showed that Cu accumulates in WI-38 HDFs just at the end of the treatment with 500 μM CuSO₄ for 16 h. This

accumulation had nearly totally disappeared 72 h later. The accumulation of Cu is transient and eightfold higher in WI-38 HDFs treated with CuSO₄ while it was constant and close to only twofold in RS. We did not observe a large difference in the accumulation of lipofuscin after the incubation, perhaps due to the fact that Cu accumulation was transient.

Fig. 6 Phosphorylation of p38^{MAPK} is implicated in CuSO₄-induced premature senescence. **a** Western blot analysis of Phospho-p38^{MAPK} just after the end of the treatment with 0 (CTL) or 500 μM CuSO₄ and with 50 mM mannitol or not for 16 h. α-Tubulin was used as control loading. WI-38 HDFs treated with 500 μM H₂O₂ for 2 h were used as positive control. **b** Western blot analysis of Hsp70, HO-1, NQO1 (1) and Nrf2 (2) just after the end of the treatment with 0 (CTL) or 500 μM CuSO₄ and with 20 μM of p38^{MAPK} inhibitor SB203580 or not for 16 h. Ten microgrammes of proteins from whole cell homogenate (1) or from the nuclear or cytoplasmic fractions (2) are used for the analysis. α-Tubulin and lamin-B were used as control loading. **c** DNA binding of Nrf2 just after the end of the treatment with 0 (CTL) or 500 μM CuSO₄ and with 20 μM of p38^{MAPK} inhibitor SB203580 or not for 16 h using TransAM ELISA kit. The results are expressed as relative DNA binding of Nrf2 in comparison with control cells and are given as mean ± S.D. from three independent experiments. Statistical analysis: Student's *t* test, *n.s.* non-significant ($P > 0.05$); $*0.05 > P > 0.01$. **d** Percentage of SA-βgal positive and percentage of cellular proliferative potential (incorporation of [³H]-thymidine) in WI-38 HDFs at 72 h after the end of the treatment with 500 μM CuSO₄ or not and with 20 μM of p38^{MAPK} inhibitor SB203580 or not for 16 h. The results are expressed in percentage and are given as mean ± S.D. from three independent experiments. The numbers in the chart represent ratios between CTL and CuSO₄-treated cells and are given as mean ± S.D. from three independent experiments. Statistical analysis was carried out with the Student's *t* test. $*0.05 > P > 0.01$; $**0.01 > P > 0.001$; $***P < 0.001$. The symbol Δ represents a statistical analysis between ratios

The results obtained on the induction of SIPS with CuSO₄ suggest that a transient increase can be sufficient to launch the process of senescence. Indeed we showed that SIPS is induced at 72 h after the end of the treatment with 500 μM CuSO₄ for 16 h, with an enlarged and flattened cell morphology typical of senescent HDFs, an increase of the proportion of SA-βgal-positive HDFs and a decreased proliferative potential. The increase of SA-βgal activity was shown to be a reliable marker of senescence in fibroblasts (Dimri et al. 1995). We demonstrated that sublethal treatment with CuSO₄ induces the significant increased abundances of the mRNA of p21^{Waf1}, p16^{ink4a}, TGF-β1, apolipoprotein J and fibronectin. We observed also the increased abundances of the mRNA of CTGF, IGFBP3, but the statistical analysis showed that these variations are not significant. All these genes are known to be overexpressed in senescent HDFs (Pascal et al. 2005). In our model, there was no increased abundance of the mRNA of osteonectin. Osteonectin is known to be a Cu-binding protein and this association seems to play a

protective role against stress-induced apoptosis (Weaver et al. 2008). It is possible that Cu perturbs osteonectin expression independently of senescence. In 2012, Matos et al. confirmed that Cu induces premature senescence in WI-38 HDFs (Matos et al. 2012). They showed the morphological changes, an increase of the proportion of SA-βgal-positive cells, growth arrest and overexpression of p21^{waf-1}, apolipoprotein J, TGF-β1, fibronectin, IGFBP3 and hemoxygenase-1 in cells treated with 250 μM CuSO₄ for 24 h, at 72 h after the end of the treatment.

We showed that CuSO₄ induces an increase of ROS production and an increase of 8-oxodG. Metals such Cu and Fe are able to induce an accumulation of DNA damage. Indeed, these metals inhibit the base excision activity of a family of DNA glycosylases by oxidizing them, changing their structure and inhibiting their binding to downstream repair proteins (Hegde et al. 2011). These mechanisms could participate in the process of growth arrest. Indeed increased ROS production and increased concentration of 8-oxodG were shown in RS (Chen et al. 1995). Nrf2 is the key transcription factor regulating the antioxidant response (Nguyen et al. 2009). We observed that CuSO₄ induces an increase of Nrf2 mRNA and a nuclear translocation of Nrf2 just after 16 h of treatment with 500 μM CuSO₄. CuSO₄ also induces an increased level of mRNA and protein of two target genes of Nrf2, NQO1 and HO-1. We demonstrated an increase of DNA binding activity for Nrf2 in cells treated with CuSO₄ suggesting that the Nrf2 pathway is induced by Cu. We can conclude that incubation with CuSO₄ induces a ROS production and an antioxidant response. The presence of antioxidants (mannitol or trolox) decreased the ROS production and the antioxidant response induced by CuSO₄. These results suggested that antioxidants are effective in abolishing oxidative stress induced by Cu. The fact that the presence of antioxidants decreases the antioxidant response probably means that their presence has resulted in a decrease of ROS production and therefore the disappearance of oxidative stress caused by Cu.

The typical senescent morphology (data not shown), the increase of SA-βgal and the irreversible growth arrest in cells treated with CuSO₄ were partially abolished by mannitol. Unlike mannitol, Cu and trolox together generated an increase in cell mortality. Thus, we used trolox only after the end of the treatment with CuSO₄, and this partially abolished the

same biomarkers. These results suggest that CuSO₄-induced oxidative stress is involved in these CuSO₄-induced biomarkers. Oxidative stress might also perturb the homeostasis of metals, causing their accumulation. In 2004, Killilea et al. confirmed that a low dose of H₂O₂ induces premature senescence in IMR-90 fibroblasts. Concomitantly, there was an acceleration of iron accumulation (Killilea et al. 2004) and thus possibility for enhancement and/or prolongation of oxidative stress and vice versa suggesting a cycling phenomenon. Metals and ROS are known to be close interactants (Jomova and Valko 2011).

Phosphorylation of p38^{MAPK} was less important when mannitol was added during Cu treatment, suggesting that the CuSO₄-induced oxidative stress is involved in the activation of p38^{MAPK}. Since p38^{MAPK} is implicated in oxidative stress response (Sun et al. 2009), we tested whether p38^{MAPK} plays a role in CuSO₄-induced oxidative stress response using a selective inhibitor of p38^{MAPK} activity. The abundance of Hsp70 and HO-1, involved in oxidative stress response, was decreased in the presence of the inhibitor of p38^{MAPK}. The expression of Hsp70 is described as dependent of p38^{MAPK} (Uehara et al. 1999).

A link between the Nrf2 and p38^{MAPK} pathway is described in different areas (Du et al. 2011). In our model NQO1 abundance, nuclear abundance and DNA binding of Nrf2 did not change in the presence of the p38^{MAPK} inhibitor, suggesting that p38^{MAPK} is not implicated upstream from Nrf2. These results suggest that the Nrf2 pathway and the p38^{MAPK} pathway were induced by CuSO₄ in parallel.

The typical morphology, the increase of SA-βgal and the decrease of proliferative potential of cells treated with CuSO₄ were partially abolished by the specific inhibitor of p38^{MAPK}. Phosphorylation of p38^{MAPK} seems to be implicated in CuSO₄-induced premature senescence of WI-38 HDFs. Zdanov et al. showed that p38^{MAPK} is involved in premature senescence of IMR-90 HFDs and regulates the expression level of many genes involved in DNA synthesis/cell cycle, heat shock response but also CTGF and IGF1P-2, -3, -5. The results obtained with the chemical inhibitor of p38^{MAPK} and with a specific siRNA for p38^{MAPK} were similar for this study (Zdanov et al. 2006).

In conclusion, we demonstrated that oxidative stress induced by CuSO₄ is partially involved in the appearance of biomarkers of senescence. We can assume that copper accumulation in senescent cells might contribute

to the development of senescence. We suspect that accumulation of Cu takes place gradually, progressively increasing oxidative stress, decreasing the effectiveness of repair and degradation systems namely DNA repair and proteolysis by the proteasome, and generating a progressive accumulation of damage. This supports the view that “Aging is the outcome of a balance between damage and repair. The rate of aging and the appearance of age-related pathology are modulated by stress response and repair pathways that gradually decline, including the proteostasis and DNA damage repair networks and mitochondrial respiratory metabolism” (Haigis and Yankner 2010). In the particular case of copper-induced premature senescence, we can hypothesize that this balance between damage and protection/repair relies, on one hand, on the ROS-induced activation of p38^{MAPK}, which is known as a strong inducer of premature senescence in human proliferative cell types and is also partly responsible for the activation of genes encoding components involved in antioxidative defences like Hsp70 and HO-1, and on the other hand, by the potential ROS-induced (or other unknown Cu-inducer) activation of Nrf-2, which in turn activates protective proteins like Hsp70, HO-1 and NQO1 probably allowing concomitant cell survival and the appearance of premature senescence.

Acknowledgments E. Boilan is a recipient of “Fonds de la Recherche dans l'industrie et l'agriculture (FRIA)”, Belgium. O. Toussaint and F. Debacq-Chainiaux are senior research associate and research associate of the FNRS, Belgium, respectively. We acknowledge the “Direction Générale Opérationnelle de l'Économie, de l'Emploi et de la Recherche” (DGO6) of the Public Service of Wallonia (SPW) for the “Nanotoxicology” Excellence Pole of Research, convention #516252 project. We thank the European Commission for Integrated Project “PROTEOMAGE”, contract FP6-518230 and infrastructure “QNano” contract INFRASTRUCTURE-2010-1-262163. We thank D.W. Domaille and C.J. Chang, Department of Chemistry and Howard Hughes Medical Institute, University of California, Berkeley, USA, for the CS1 probe. We thank J-F. Colomer, C. Charlier and D. Delgleize from Service of Electronic Microscopy, FUNDP, Namur, Belgium for the help and advice in TEM and EDX.

References

- Borghouts C et al (2001) Copper-modulated gene expression and senescence in the filamentous fungus *Podospora anserina*. *Mol Cell Biol* 21(2):390–399
- Borghouts C, Osiewicz HD (1998) GRISEA, a copper-modulated transcription factor from *Podospora anserina*

- involved in senescence and morphogenesis, is an ortholog of MAC1 in *Saccharomyces cerevisiae*. *Mol Gen Genet* 260(5):492–502
- Brewer GJ (2007) Iron and copper toxicity in diseases of aging, particularly atherosclerosis and Alzheimer's disease. *Exp Biol Med* (Maywood, NJ) 232(2):323–335
- Campisi J, d'Adda di Fagnana F (2007) Cellular senescence: when bad things happen to good cells. *Nat Rev Mol Cell Biol* 8(9):729–740
- Chen Q et al (1995) Oxidative DNA damage and senescence of human diploid fibroblast cells. *Proc Natl Acad Sci U S A* 92(10):4337–4341
- Debaq-Chainiaux F et al (2010) p38(MAPK) in the senescence of human and murine fibroblasts. *Adv Exp Med Biol* 694:126–137
- Desesso JM, Scialli AR, Goeringer GC (1994) D-mannitol, a specific hydroxyl free radical scavenger, reduces the developmental toxicity of hydroxyurea in rabbits. *Teratology* 49(4):248–259
- Dimri GP, Lee X, Basile G, Acosta M, Scott G, Roskelley C et al (1995) A biomarker that identifies senescent human cells in culture and in aging skin in vivo. *Proc Natl Acad Sci U S A* 92(20):9363–9367
- Du Z-X et al (2011) Proteasome inhibition induces a p38 MAPK pathway-dependent antiapoptotic program via Nrf2 in thyroid cancer cells. *J Clin Endocrinol Metab* 96(5):E763–E771
- Gredilla R, Grief J, Osiewacz Heinz D (2006) Mitochondrial free radical generation and lifespan control in the fungal aging model *Podospora anserina*. *Exp Gerontol* 41(4):439–447
- Haigis MC, Yankner BA (2010) The aging stress response. *Mol Cell* 40(2):333–344
- Hayflick L, Moorhead PS (1961) The serial cultivation of human diploid cell strains. *Exp Cell Res* 25:585–621
- Hegde ML et al (2011) Oxidative genome damage and its repair in neurodegenerative diseases: function of transition metals as a double-edged sword. *J Alzheimer's Dis: JAD* 24(Suppl 2):183–198
- Höhn A et al (2010) Lipofuscin-bound iron is a major intracellular source of oxidants: role in senescent cells. *Free Radic Biol Med* 48(8):1100–1108
- Jomova K, Valko M (2011) Advances in metal-induced oxidative stress and human disease. *Toxicology* 283(2–3):65–87
- Jung T, Höhn A, Grune T (2010) Lipofuscin: detection and quantification by microscopic techniques. In: Armstrong DD (ed) *Advanced protocols in oxidative stress II*. Humana Press, Totowa, pp 173–193
- Kang KW, Lee SJ, Kim SG (2005) Molecular mechanism of Nrf2 activation by oxidative stress. *Antioxid Redox Signal* 7(11–12):1664–1673
- Killilea DW et al (2004) Iron accumulation during cellular senescence. *Ann N Y Acad Sci* 1019(1):365–367
- Mansouri A et al (1997) Premature oxidative aging of hepatic mitochondrial DNA in Wilson's disease. *Gastroenterology* 113(2):599–605
- Matos L, Gouveia A, Almeida H (2012) Copper ability to induce premature senescence in human fibroblasts. *Age (Dordr)* 34(4):783–794
- Motonishi S et al (2006) Copper- and iron-rich matrices in hepatocellular lipofuscin particles of a young male patient: diagnostic ultrastructures for Wilson disease. *Ultrastruct Pathol* 30(6):409–414
- Nguyen T, Nioi P, Pickett CB (2009) The Nrf2-antioxidant response element signaling pathway and its activation by oxidative stress. *J Biol Chem* 284(20):13291–13295
- Osiewacz HD, Borghouts C (2000) Cellular copper homeostasis, mitochondrial DNA instabilities, and lifespan control in the filamentous fungus *Podospora anserina*. *Exp Gerontol* 35(6–7):677–686
- Pascal T et al (2005) Comparison of replicative senescence and stress-induced premature senescence combining differential display and low-density DNA arrays. *FEBS Lett* 579(17):3651–3659
- Remacle J et al (1995) Low levels of reactive oxygen species as modulators of cell function. *Mutat Res* 316(3):103–122
- Scheckhuber CQ et al (2009) Age-related cellular copper dynamics in the fungal ageing model *Podospora anserina* and in ageing human fibroblasts. *PLoS One* 4(3):e4919
- Seth R et al (2004) In vitro assessment of copper-induced toxicity in the human hepatoma line, Hep G2. *Toxicol Vitro* 18(4):501–509
- Simmons SO et al (2011) NRF2 oxidative stress induced by heavy metals is cell type dependent. *Curr Chem Genom* 5:1–12
- Stern BR (2010) Essentiality and toxicity in copper health risk assessment: overview, update and regulatory considerations. *J Toxic Environ Health A* 73(2):114–127
- Sun Z, Huang Z, Zhang DD (2009) Phosphorylation of Nrf2 at multiple sites by MAP kinases has a limited contribution in modulating the Nrf2-dependent antioxidant response. *PLoS One* 4(8):e6588
- Terman A et al (2010) Mitochondrial turnover and aging of long-lived postmitotic cells: the mitochondrial-lysosomal axis theory of aging. *Antioxid Redox Signal* 12(4):503–535
- Toussaint O, Medrano EE, von Zglinicki T (2000) Cellular and molecular mechanisms of stress-induced premature senescence (SIPS) of human diploid fibroblasts and melanocytes. *Exp Gerontol* 35(8):927–945
- Uehara T et al (1999) Possible involvement of p38 MAP kinase in HSP70 expression induced by hypoxia in rat primary astrocytes. *Brain Res* 823(1–2):226–230
- Vasudevaraju P et al (2010) New evidence on iron, copper accumulation and zinc depletion and its correlation with DNA integrity in aging human brain regions. *Indian J Psychiatry* 52(2):140–144
- Weaver MS, Workman G, Sage EH (2008) The copper binding domain of SPARC mediates cell survival in vitro via interaction with integrin β 1 and activation of integrin-linked kinase. *J Biol Chem* 283(33):22826–22837
- Zatta P et al (2008) Accumulation of copper and other metal ions, and metallothionein I/II expression in the bovine brain as a function of aging. *J Chem Neuroanat* 36(1):1–5
- Zdanov S et al (2006) Identification of p38MAPK-dependent genes with changed transcript abundance in H₂O₂-induced premature senescence of IMR-90 hTERT human fibroblasts. *FEBS Lett* 580(27):6455–6463
- Zeng L, Miller EW, Pralle A, Isacoff EY, Chang CJ (2006) A selective turn-on fluorescent sensor for imaging copper in living cells. *J Am Chem Soc* 128(1):10–11